PARTICLE FLUXES IN THE NW IBERIAN COASTAL UPWELLING SYSTEM: HYDRODYNAMICAL AND BIOLOGICAL CONTROL

Zúñiga, D.[a,d 1*], Villacieros-Robineau, N.[b], Salgueiro, E.[c,e], Alonso-Pérez, F.[a], Rosón, G.[d], Abrantes, F.[c,e], Castro, C.G.[a]

[a] Consejo Superior de Investigaciones Científicas (CSIC), Instituto de Investigaciones Marinas (IIM), E-36208, Vigo, Spain

[b] Université Pierre et Marie Curie, Laboratoire d'Océanographie et du Climat, 75005, Paris, France

[c] Instituto Português do Mar e da Atmosfera (IPMA), Div. Geologia e Georecursos Marinhos, 1749-077, Lisbon, Portugal

[d] Universidad de Vigo, Departamento de Física Aplicada, Campus Lagoas-Marcosende, E-36310, Vigo, Spain

[e] CCMAR - Centre of Marine Sciences. Universidade do Algarve, Campus de Gambelas, 8005-139 Faro

[1] present address: Universidad de Vigo, Departamento de Física Aplicada, Campus Lagoas-Marcosende, E-36310, Vigo, Spain

*corresponding autor: diana.zuniga@uvigo.es (Zúñiga, D.), Tel.: +34 986 812 644, Fax: +34 986 813 792. Universidad de Vigo, Departamento de Física Aplicada, Campus Lagoas-Marcosende, E-36310, Vigo, Spain

Abstract

To better understand sources and transport of particulate material in the NW Iberian coastal upwelling system, a mooring line dotted with an automated PPS 4/3 sediment trap was deployed off Cape Silleiro at the base of the photic zone. The samples were collected from November 2008 through June 2012 over sampling periods of 4-12 days.

Our study represents the first automated sediment trap database for the NW Iberian margin. The magnitude and composition of the settling material showed strong seasonal variability with

the highest fluxes during the poleward and winter mixing periods (averages of 12.9 ± 9.6 g m^{-2} d^{-1} and 5.6 ± 5.6 g m^{-2} d^{-1} respectively), and comparatively lower fluxes (3.6 ± 4.1 g m^{-2} d^{-1}) for the upwelling season. Intensive deposition events registered during poleward and winter mixing periods were dominated by the lithogenic fraction (80±3%). They were associated to high energy wave-driven resuspension processes, due to the occurrence of south-westerly storms, and intense riverine inputs of terrestrial material from Minho and Douro rivers.

On the other hand, during the spring - summer upwelling season, the share of biogenic compounds (organic matter, calcium carbonate (CaCO3), biogenic silica (bSiO2)) to downward fluxes was higher, reflecting an increase in pelagic sedimentation due to the seasonal intensification of primary production and negligible river inputs and wave-driven resuspended material. Otherwise, the large variations of biogenic settling particles were mainly modulated by upwelling intensity, which by means of upwelling filaments ultimately controlled the offshore transport of the organic carbon fixed by primary producers towards the adjacent ocean. Based on the average downward flux of organic carbon (212 mg C m^{-2} d^{-1}) and considering an average primary production of 1013 mg C m^{-2} d^{-1} from literature, we estimated that about 21% of the fixed carbon is vertically exported during the upwelling season.

Keywords: particle fluxes; resuspension; particulate organic carbon; filament; coastal upwelling; NE Atlantic

1. INTRODUCTION

Continental margins, especially those affected by coastal upwelling are characterized by high primary production rates (Chavez et al., 2011; Bauer et al., 2013). These areas, representing the transition zone between the land and the open ocean are also strongly affected by seasonality of atmospheric regimes, which ultimately control additional terrestrial inputs to the system and convert these areas in regions of high particulate matter concentration. The identification of sources and transport pathways of particulate matter in these highly-productive coastal upwelling systems is essential to: (i) tackle particle flux transfer between the shelf and the deep ocean, and (ii) to discern which fraction of the particulate organic carbon may be attributed to primary production, a fundamental issue to be resolved in order to understand global ocean carbon cycling (Wollast, 1998; Muller-Karger et al., 2005; Liu et al., 2010).

Since the 80s, vertical particle fluxes have been largely studied, as they represent the missing link between the processes affecting particulate material at sea surface and their routes towards the deep ocean. Some global (e.g. JGOFS) and regional projects attempted to understand seasonal and inter annual organic carbon export rates in different ocean basins (Martin et al., 1987; Antia et al., 2001; Armstrong et al., 2002; Francois et al., 2002; Lutz et al., 2002; Goñi et al., 2003; Honjo et al., 2008). Most of these studies have been focused on oceanic waters where the characteristics of particle fluxes are affected by the seasonality of large-scale oceanographic and biogeochemical processes, mainly linked to primary production annual cycle. Nevertheless, downward flux studies on continental margins where additional particle sources mask pelagic sedimentation showed how the particles export is greatly variable both in space and time. This large variability is mainly due to hydrodynamic processes such as waves and/or strong currents that favour resuspension of surface sediments (e.g. Biscaye and Anderson, 1994; Peña et al., 1996; Heussner et al., 2006). Besides, in highly productive coastal upwelling systems, sediment trap studies have evidenced a decoupling between primary production and particulate organic carbon flux at the base of the photic zone (e.g. Pilskaln et al., 1996; Thunell, 1998; Peña et al., 1996; Fisher et al., 2009;). These authors proposed a variety of physical and biological factors determining the export rates of organic carbon during the

upwelling season, emphasizing the role of particulate organic recycling rates and offshore advection of organic material.

The NW Iberian coast is located at the northern boundary of the unique upwelling regime in Europe, the Iberian-Canary Upwelling System (Fraga, 1981, Arístegui et al., 2009). This system has a particular set of physical and chemical characteristics, favouring blooms of phytoplankton that lead to high secondary production, maintaining large stocks of economically important exploitable species. Many biogeochemical aspects of the NW Iberian upwelling system have recently been studied, such as CO_2 spatial and temporal variability (Gago et al., 2003), biogeochemistry of the water column (Castro et al., 2000), dynamics of the dissolved organic matter (Álvarez-Salgado et al., 1999), phytoplankton community structure (Figueiras and Ríos, 1993; Espinoza-Gonzalez et al., 2012) and benthic – pelagic coupling (Alonso-Pérez et al., 2010). However, very few studies have been focused on the vertical sinking of organic material, covering short periods of time (<1month) and by means of multitraps collector systems (Bode et al., 1998; Olli et al., 2001; Varela et al., 2004; Zúñiga et al., 2011).

In this context, this work focuses on the downward particle fluxes in the NW Iberian coastal upwelling system using the first long-term sequential sediment trap data collected in this region. Biogeochemical data for sediment trap samples are combined with oceanographic observations to examine how hydrodynamic and biological factors determine the seasonal variation of magnitude and geochemical composition of settling particulate material. This study will also help us to understand how this upwelling dominated continental shelf concentrate and/or export organic carbon to the open ocean.

2. METHODS

2.1. Study area

Our station (RAIA) is located on the NW Iberian continental shelf off Cape Silleiro (42º 05´ N; 8º 56´ W) at 75 m water depth (Figure 1). The wind regime in this coastal upwelling region shows a clear seasonal signal (Wooster et al., 1976). During spring - summer (April to September - October), the NW Iberian coast is characterized by prevailing northerly winds, that cause upwelling of cold and nutrient rich subsurface Eastern North Atlantic Central Water (ENACW) on the shelf and into the Rías Baixas, triggering the high primary production of the region (Fraga,

1981; Tenore et al., 1995). The establishment of northerly winds favour the formation of upwelling filaments (Haynes et al. 1993) that stretch offshore, potentially exporting organic matter to the adjacent ocean (Alvarez-Salgado et al., 2001). By contrast, during autumn – winter (October to March – April), south-westerly winds favour coastal downwelling and the northward advection of warm, saline and nutrient-poor southerly waters conveyed by the Iberian Poleward Current (IPC) (Haynes and Barton, 1990, Castro et al., 1997). This poleward flow confines coastal waters over the shelf, precluding shelf-ocean exchange (Castro et al., 1997; Alvarez-Salgado et al., 2003; Schmidt et al., 2010). With the winter cooling (usually February - March), surface waters temperature drop and winter mixing occurs, resulting in a well homogenized mixed layer of cold and nutrient rich waters in the adjacent ocean (Álvarez–Salgado et al., 2003; Castro et al., 2006). On the other hand, these south-westerly winds during the autumn-winter promote significant wave heights exceeding 5 m 1.46% the time (mean annual conditions) and with a related peak period between 14 s and 18 s. The highest values of maximum wave height measured in the area achieved 16.3 m. Such stormy conditions cause sediment remobilization on the continental shelf (Dias et al., 2002; Vitorino et al., 2002; Villacieros-Robineau et al. (unpublished results)).This fact explains the characteristics of the bottom seafloor in the area of Cape Silleiro where surface sediments mainly consist in rocks and in minor proportion muddy sands (Dias et al 2002). The NW Iberian continental shelf is also subject to river inputs, mainly from the Douro and Minho rivers. The annual average discharges are about 550 and 310 $m^3 s^{-1}$ for the Douro and Minho rivers respectively, and show strong seasonality. Maximum river inflows (up to 3850 $m^3 s^{-1}$ for Douro river and 1800 $m^3 s^{-1}$ for Minho river) occurred during winter months and minima (less than 200 $m^3 s^{-1}$) during summer (Dias et al., 2002, Otero et al., 2010).

2.2. Sampling strategy

A mooring line equipped with an automated Technicap PPS 4/3 sediment trap at 35 m of water depth and a CTD-SBE19 plus 2 m below the trap was used to monitored RAIA station from November 2008 to June 2012 (Figure 2 and Table 1). Unfortunately some data were lost due to technical problems and bad weather conditions (see Table 1). In addition, monthly cruises at RAIA station onboard R/V Mytilus were carried out in order to i) characterize the water column by conducting profiles for recording temperature and salinity (CTD-SBE25) and ii) collect

142 discrete water column samples (5, 10, 20, 35, 50, 65 m) by means of an oceanographic rosette
143 provided with 10-L PVC Niskin bottles for the determination of inorganic nutrients and
144 chlorophyll *a* (Chl *a*).
145
146 **2.3. Physical forcing**
147 Daily Ekman transport ($-Q_x$), an estimate of the volume of water upwelled per kilometre of coast,
148 was calculated according to Bakun´s (1973) method:
149 $-Q_x = -((\rho_a C_D |V|)/(f \rho_{sw}))\, V_y$
150 where ρ_a is the density of the air (1.22 kg m^{-3}) at 15 ºC, C_D is an empirical dimensionless drag
151 coefficient (1.4 10^{-3}), f is the Coriolis parameter (9.76 10^{-5}) at 42 ºN, ρ_{sw} is the seawater density
152 (1025 kg m^{-3}) and |V| and V_y are the average daily module and northerly component of the
153 geostrophic winds centred at 42º N, 10º W, respectively. Average daily winds were estimated
154 from surface atmospheric pressure fields (WXMAP atmospheric model) distributed by the US
155 Navy Fleet Numerical Meteorological and Oceanographic Center (FNMOC) in Monterey,
156 California (http://www.usno.navy.mil/FNMOC). Positive values show the predominance of
157 northerly winds that induces upwelling on the shelf. On the contrary, negative values indicate
158 the existence of downwelling processes. Minho and Douro river discharges were obtained from
159 the web site https://github.com/PabloOtero/uptodate_rivers (Otero et al., 2010). Time series of
160 wave data were done using the available data from WANA hindcast reanalysis points 3027034
161 ($WANA_S$: off Silleiro (42º 15'N; 9º W)) and 1044067 ($WANA_G$: off A Guarda (41º 45´N; 9º W))
162 (Figure 1). Data were supplied by Puertos del Estado.
163
164 **2.4. Water column data**
165 Nutrient contents were determined by segmented flow analysis with Futura-Alliances
166 autoanalyzers following Hansen and Grassoff, (1983). The analytical error for nitrate is ± 0.05
167 µM. For Chl *a* concentration analyses, 250 mL water samples were filtered through GFF filters
168 under low vacuum. The filters were placed in tubes and immediately stored in the dark at –20 ºC
169 for 24 h. Afterwards, 10 mL of 90% acetone were added to the tubes, placed in the refrigerator
170 for 8 hours, and the extracted fluorescence read before and after acidification (Chl *a* corrected)

using a Turner Designs fluorometer calibrated with pure Chl *a* (Yentsch and Menzel, 1963). Chl *a* measurement precision is ± 0.05 µg L^{-1}.

2.5. Sediment trap processing and analytical methods

The Technicap PPS 4/3 sequential-sampling sediment trap used in this study has a cylindric–conical shape with a height/diameter ratio of 1.7 and a collecting area of 0.05 m^2 (Heussner et al., 1990). In the laboratory, the rotary collector was cleaned with a detergent, soaked in HCl 0.5 N overnight, and rinsed several times with distilled water, and once on board, traps were rinsed with seawater. The receiving cups (250 mL) were filled with brine solution (5 psu in excess) to which 6 mL of saturated mercuric chloride solution was added to avoid the degradation of the collected particles and the disruption of swimmers (including all the organisms that do not fall gravitationally through the water column). Upon recovery, the receiving cups were stored in the dark at 2 – 4 °C until processing. Once in the laboratory, swimmers were removed from the samples by using fine tweezers under a dissecting microscope. Subsequently, samples were split into 5 aliquots using a high precision McLane WSD-10 sample divider. Each aliquot was rinsed with cold distilled water to remove the salts and then centrifuged to eliminate the supernatant. This procedure was repeated for three/four times to ensure that the sample was completely salt free. Aliquots were stored at -80 ºC and freeze-dried.

Total mass was gravimetrically determined. After that, for major compound and isotopic analyses, samples were ground to a fine powder. For total and organic carbon (C_{org}) and nitrogen elemental composition analysis, 20 mg subsamples of dry sediment were used. Subsamples for organic carbon were firstly decarbonated with repeated additions of 10 µL of HCl 25%. Total and organic carbon and nitrogen were measured with a Perkin Elmer 2400 CNH analyser. The precision of the method is ± 0.3 µmol C L^{-1} and ± 0.1 µmol N L^{-1}, respectively.

Organic carbon isotopic ($\delta^{13}C_{org}$) analyses were performed over ~15 mg of decarbonated sample in silver capsules. Samples were measured by continuous flow isotope ratio mass spectrometry using a Thermo Finnigan MAT253 mass spectrometer coupled to an elemental analyser Carlo Erba EA1108 through a Conflo III interface. Organic carbon isotope composition is expressed as $\delta^{13}C_{org}$ parts per thousand (‰) relative to VPDB (Vienna Pee Dee Belemnite). Assuming that all the inorganic carbon was constituted by calcium carbonate ($CaCO_3$), the

201 organic matter (OM) was calculated as [C_{org} × 1.87] and the $CaCO_3$ content as [(total carbon–
202 C_{org}) × 8.33] (Fraga et al., 1998).
203 Biogenic opal ($bSiO_2$) content was analysed following Mortlock and Froelich (1989). The
204 samples were treated with 2M Na_2CO_3 for 5 h at 85ºC to extract the silica and then measured
205 as dissolved silica by colorimetric reaction. The value of Si concentration was converted into
206 $bSiO_2$ after multiplying it by a factor of 2.4 (Mortlock and Froelich, 1989).
207 The lithogenic fraction of each sediment trap sample was obtained by the difference between
208 the total mass and the sum of the biogenic compounds (OM, $CaCO_3$ and $bSiO_2$).
209

210 **2.5.1. Sediment trap collection efficiency**

211 Sediment trap time series constitute the best way to study the variations of vertical particulate
212 matter fluxes in the ocean. However, some studies point out that they may be subjected to
213 some biases, depending on trap design, current velocity and characteristics of the settling
214 particles. In this sense, Gardner et al. (1997) concluded that at current speeds less than 22 cm
215 s^{-1} vertical fluxes measured with cylindrical traps are not affected by horizontal currents. For the
216 sampling period November 2008- May 2010, current speeds were registered by an upwards
217 looking bottom mounted Doppler current profiler at RAIA location. Mean statistical parameters
218 at 45 m water depth are presented in Table 2. Current velocities were lower than 22 cm s^{-1} for
219 94%, 85% and 76% of the time during upwelling, poleward and winter mixing periods,
220 respectively. Likewise, tilt calculated from examination of CTD pressure data mounted 2 m
221 below the sediment trap also showed that the mooring line tilting was reduced, even during
222 strong current episodes (Table 2). Thus, we assume that our sediment trap was not affected by
223 hydrodynamical biases during most of the time that it was deployed.
224

225 **3. RESULTS**

226 **3.1. Oceanographic conditions**

227 Prevailing south-westerly winds (negative $–Q_x$ values) were registered from October to April-
228 May causing strong downwelling conditions. (Figure 3a). Such conditions were accompanied by
229 strong SW storms responsible for significantly high wave heights (H_S) (up to 9.1 m) (Figure 3c).
230 Wave action lead to resuspension of bottom sediments as reflected by the significant increase

231 in deep water column turbidity under stormy conditions (Figure 4e).At the same time, intense
232 Minho and Douro river discharges (> 400 m^3 s^{-1}), left their imprint as low salinity (< 35.6) and
233 relatively high nitrate content water lens at sea surface (Figure 4b, 4b, 4e).
234 Hydrographically, from late autumn (October) to early winter (January) downwelling conditions
235 corresponded with the presence of the Iberian Poleward Current (IPC) in the region, as
236 indicated by the anomalously warm (15-16 ºC) and salty (>35.8) waters with relatively low
237 nutrient (2-4 µmol kg^{-1}) and Chl *a* (< 1 mg m^{-3}) contents (Figure 4). Afterwards from January to
238 March-April, the water column was thermally homogeneized (~14ºC) and characterized by high
239 nitrate levels (4-6 µmol kg^{-1}) due to the winter mixing and river runoff (Figure 3b, 4).
240 Subsequently, the transitional phase from winter to the upwelling season was marked by the
241 spring bloom episode, as registered in March 2008, April 2011 and March 2012. During these
242 spring transition periods, the development of sea surface thermal stratification due to incipient
243 solar heating, jointly with the upwelled of nutrient rich subsurface waters, caused by the
244 establishment of northerly winds, trigger the increase of Chl *a* levels in the water column (Figure
245 4). After that, between May and October a series of upwelling-relaxation cycles, as observed by
246 $-Q_x$ temporal variability (Figure 3a), promoted the upwelling of cold (<14 ºC) Eastern North
247 Atlantic Central waters (ENACW) on the continental shelf, as the shoaling of the isotherms
248 indicates (Figure 3a, 4a). This nutrient rich (10-12 µmol kg^{-1}) subsurface water mass favoured
249 the development of Chl *a* maxima, with concentrations as high as 9 mg m^{-3} , as registered in
250 July 2009 (Figure 4).
251
252 **3.2. Magnitude and timing of fluxes**
253 Time series of total mass fluxes (TMF) off Cape Silleiro revealed high values and significant
254 seasonal and inter annual variability within the whole study period (Figure 5). The highest fluxes
255 (12.9 ± 9.6 g m^{-2} d^{-1} and 5.6 ± 5.6 g m^{-2} d^{-1} for poleward and winter mixing, respectively) were
256 always recorded during autumn – winter time, whereas during spring-summer upwelling periods
257 TMF were comparatively low (3.6 ± 4.1 g m^{-2} d^{-1}), excluding the moderately intense deposition
258 events in July 2009, September 2011 and June-July 2012, when values as high as 14 g $m^{-2}d^{-1}$
259 were registered.

Temporal evolution of both biogenic (organic matter (OM), calcium carbonate ($CaCO_3$) and biogenic opal ($bSiO_2$)) and lithogenic fluxes presented similar trends, in agreement with TMF variability (Figure 5). Fluxes of OM, $CaCO_3$ and $bSiO_2$ ranged around multi-year averages of 458 ± 446 mg m^{-2} d^{-1}, 542 ± 623 mg m^{-2} d^{-1} and 263 ± 254 mg m^{-2} d^{-1}, respectively, registering higher values during the poleward and winter mixing periods (Figure 5 and Table 3). In contrast, and except for the mass biodeposition events in July 2009, September 2011 and June-July 2012, minimum OM, $CaCO_3$ and $bSiO_2$ fluxes were linked to upwelling seasons, when values below 400 mg m^{-2} d^{-1} were recorded for the three major biological compounds. Time series of lithogenic fluxes ranged around a multi-year average of 4.7 ± 5.2 g m^{-2} d^{-1}, showing clear seasonal contrasts. Two intense deposition events were recorded during November 2009 and February 2011 when fluxes were as high as 24 g m^{-2} $d^{-1}$and 23 g m^{-2} d^{-1}, respectively (Figure 5). Relative contributions of major compounds to TMF are presented in Figure 6 and Table 3. It is noteworthy that settling particulate material is mainly composed by lithogenic matter for the whole sampling period, with a mean percentage of 74.6 ± 7.8%. Seasonally, the relative contribution of the lithogenic fraction was higher during poleward and winter mixing periods than during upwelling seasons when biogenic compounds relatively increased their contribution. The percentage of OM to the settling material ranged around values of 13.2 ± 5.7% during upwelling periods. On the contrary, the contribution of OM was lower for the poleward and winter periods, ranging around mean values of 9.7 ± 4.8% and 7.7 ± 2.1%, respectively. Seasonal patterns for both %$CaCO_3$ and %$bSiO_2$, that ranged around multi-year averages of 9.3 ± 4.9% and 4.8 ± 2.0% respectively, were similar to temporal variability of %OM, with relative higher contributions during upwelling periods.

The organic carbon to total nitrogen (C_{org} /TN) atomic ratio of sinking particles also showed significant seasonal differences for the studied years, with values higher than 10 during lithogenic dominated autumn-winter events (peaks 2.7.8.10.13) and values lower than 9 for the most representative upwelling episodes (peaks 5,6,9,11,12,15; Figure 7). Organic carbon ($\delta^{13}C_{org}$) isotopic composition signal of the sinking particles ranged from -20.4‰ to -23.7‰ for the upwelling and the winter season, respectively (Figure 7).

4. DISCUSSION

290 This work represents the first multi-year particle flux dataset obtained with time-sequential
291 sediment traps within the NW Iberian continental margin. The few previous studies focused on
292 vertical fluxes have only captured short periods of time and except for the work by Bode et al.
293 (1998) off A Coruña and by Olli et al. (2001) off Cape Silleiro, all the published sediment trap
294 data were obtained inside the adjacent Rías Baixas (Varela et al., 2004, Piedracoba et al.,
295 2008, Alonso-Pérez et al., 2010, Zúñiga et al., 2011).
296 The magnitude and composition of total mass fluxes off Cape Silleiro presented abrupt changes
297 for the entire time series and showed strong seasonal variability (Figure 5). Major flux peaks
298 occurring during highly hydrodynamic downwelling seasons were ruled by the lithogenic
299 fraction. Comparatively lower fluxes with a relatively higher biogenic contribution dominated
300 during less energetic upwelling periods (Figures 2, 4, 5 and Table 3). These results indicate that
301 the hydrodynamic conditions,modulated by the upwelling / downwelling seasons, have a major
302 influence over the particulate material settling in this coastal upwelling system.
303
304 **4.1. Downwelling season: The role of surface sediment resuspension and river inputs**
305 During the poleward and winter mixing periods, south-westerly winds favoured downwelling of
306 surface oceanic waters towards the continental shelf, confining coastal waters over the shelf
307 and precluding exchange with the adjacent ocean (Castro et al., 1997, Álvarez-Salgado et al.,
308 1997; Álvarez-Salgado et al., 2003). These studies have described how the shelf –ocean
309 blocking effect caused by the presence of the Iberian Poleward Current hinders the offshore
310 export of suspended particulate organic matter, and enhances its remineralization on the inner
311 shelf. In fact, the higher amount of material collected into the sediment trap during the poleward
312 and winter mixing periods (Figures 4, Table 3) point to a prevalence of particulate matter
313 sedimentation on the inner shelf over offshore horizontal transport, in response to this blocking
314 mechanism of the coastal regime.
315 On the other hand, during these months we also observed high energy wave environment, with
316 Hs> 5m (Figure 3), caused by intense SW storms (Oliveira et al., 2002; Villacieros-Robineau et
317 al., in preparation). The waves associated with these stormy conditions produce high shear
318 velocities, constituting the main forcing mechanisms of erosion and resuspension of surface
319 sediments deposited at the inner shelf (van Weering et al. 2002, Villacieros-Robineau et al., in

preparation). In this way, we observed how large amounts of particulate material has been resuspended into the water column during autumn and winter storms, as reflected by the significant increase in deep water column turbidity (Figure 4e). This explains the coupling between the massive lithogenic flux events (peaks 2, 7, 8, 10, 13) and the high wave heights registered at the Silleiro and A Guarda buoys (Figure 8). During these high-energy episodes both lithogenic and biogenic fluxes achieved their maximum values revealing that not only lithogenic particles but also organic matter as well as silicious and calcareous shelled organisms were resuspended from surface sediments during the downwelling season.

Except for the high flux event of November 2009 (peak 7) and the period between November 2011 – March 2012, strong wave action has been accompanied by intense Minho and Douro river discharges (Figure 3). The Minho and Douro flood events had a significant effect over the thermohaline structure of the water column through the formation of cold and low salinity water lens (Figure 4b), as previously studied by Otero et al. (2010). River discharges constitute an additional source of lithogenic and terrestrial organic matter to the sediment trap resulting from the bulk of sediment washed out from the rivers onto the continental shelf (Figure 3, 6 and 7), as proposed by Dias et al. (2002). Thus, the marked co-ocurrence and seasonality of these two factors, i.e. river discharges and sediment resuspension, clearly modulated the amount and quality of the material collected into the sediment trap during poleward and winter mixing periods.

The temporal evolution of C_{org}/TN ratio and $\delta^{13}C_{org}$ allowed an analysis of the quality of the settling material (Figure 7). The C_{org}/TN ratios (9.9 ± 0.8) during poleward and winter mixing periods, significantly higher than the classical Redfield ratio for marine plankton (6.7) (Redfield, 1958) pointed to more refractory organic matter being captured by our sediment trap. This fact is also corroborated by $\delta^{13}C_{org}$ displaying values clearly lighter (-23.29 ± 0.34‰) than the typical pelagic organic matter end-member for the adjacent Rías Baixas (-19.56 ± 2.01‰) (Filgueira and Castro, 2011). Moreover, $\delta^{13}C_{org}$ during these massive deposition events was similar to the $\delta^{13}C_{org}$ signal for surface sediments of the NW Iberian inner shelf found by Schmidt et al. (2010), suggesting that remobilization of underlying sediments during autumn and winter storm events may provide of more degraded organic matter to the settling material. At this point, one intriguing question comes from the fact that our carbon isotopic values may also be the result of

350 a mixture between the marine $\delta^{13}C_{org}$ characteristic value and the lighter river terrestrial organic
351 matter end-member (-26.2‰ for Minho river; from Schmidt et al., 2010). The observed decrease
352 of carbon isotopic composition of the sediment trap material could also be a direct evidence of
353 how river flows may also leave their imprint in the particulate matter sinking at the inner shelf.
354 From all these observations, we assume that even it is not possible to discern between organic
355 matter from river inputs and surface sediment resuspension, there must be a large contribution
356 of terrestrial organic carbon from these two sources in the trap material. Our results also
357 corroborate previous physical and sedimentological studies that described this continental
358 margin as a highly hydrodynamic region, where river discharges and winter storms play a key
359 role in the distribution of fine sediment in the inner shelf (Vitorino et al., 2002; Schmidt et al.,
360 2010).
361
362 **4.2. Upwelling season: primary flux and carbon export**
363 From March - April to September - October, northerly winds promote upwelling favourable
364 conditions that lead to increases in primary production, reaching the highest annual values and
365 representing about 63% of the total annual net primary production (Joint et al 2001). The time
366 series of Chl *a* off Cape Silleiro, as an estimate of phytoplankton biomass, followed this
367 seasonal pattern (Figure 4). Taking into account this high phytoplankton biomass, and the low
368 wave energy conditions and negligible river discharges (Figure 3) during this period, it could be
369 expected to find high vertical biogenic fluxes. However, we observed a large variability in the
370 biogenic fluxes during this season, mainly modulated by upwelling intensity (Figure 9). It is well
371 established that strong northerly winds may contribute to the oceanwards transport of a large
372 fraction of the biogenic particles from the continental shelf by means of upwelling filaments
373 formation (Suess, 1980; Walsh, 1981; Thunell, 1998; Olli et al., 2001). Off Cape Ghir, García-
374 Muñoz et al (2005) concluded that about 63% of the average annual primary production for the
375 region is susceptible to be exported offshore via water filament formation. For the NW Iberian
376 shelf, Alvarez-Salgado et al. (2001) estimated that the resultant organic carbon export by
377 upwelling filaments may represent as much as 45% of the total annual primary production,
378 including both dissolved and particulate organic carbon. The variability observed on the vertical
379 fluxes of C_{org} during the upwelling season seems to respond in this way, as shown in Figure 9.

380 During events 4, 6, 9 and 11, intense Ekman transport probably caused the formation of
381 upwelling filaments, favouring the horizontal offshore export of the fixed organic carbon over
382 vertical export, resulting in relatively low C_{org} vertical fluxes. Under relatively low Ekman
383 transport, the offshore export is not so favoured over the vertical one, registering high values of
384 C_{org} vertical fluxes as occurred for events 1, 5, 12 and 15. The highest C_{org} vertical fluxes were
385 reached in June – July 2009 (event 5) under a relaxation of northerly winds and high Chl *a*
386 levels, leading to a C_{org} vertical export as high as 866 mg C m^{-2} d^{-1}.
387 If we consider the average net primary production value of 1013 mg C m^{-2} d^{-1} during the
388 upwelling season reported by Joint et al. (2001) and take into account that the average C_{org} flux
389 from the sediment trap data for the upwelling season was 212 mg C m^{-2} d^{-1}, we estimate that in
390 seasonal terms about 21% of the primary production is vertically exported from the photic zone
391 in this coastal upwelling area. This value is similar to the range of 14-26 % obtained by Olli et al.
392 (2001) from a lagrangian experiment carried out in the Iberian continental shelf during a
393 summer upwelling season.
394 On the other hand, the time series of sediment trap material collected off Cape Silleiro also
395 revealed that the contribution of biogenic material to total mass during upwelling season was
396 on average (30 ± 7%), higher than during the downwelling (poleward: 20±3%; mixing: 19±3%)
397 periods (Table 3). Besides, the lower C_{org}/TN ratio and the high carbon isotopic signal ($\delta^{13}C_{org}$>-
398 21‰) corroborate that biogenic particle fluxes are derived from recently formed organic matter
399 by primary producers (Figure 7 and Table 3).
400 The high positive correlation between C_{org} fluxes and both $CaCO_3$ and $bSiO_2$ fluxes (r=0.96 and
401 r=0.96, respectively) during the upwelling season, higher than the correlation with lithogenic
402 fluxes (r=0.90), also point to the overall control that both silicious (diatoms) and calcareous
403 (coccolithopheres) phytoplankton communities exert over C_{org} vertical export in the NW Iberian
404 coastal upwelling system (Table 4). These correlation coefficients are very similar to those
405 obtained for other upwelling-dominated continental margins (Thunell et al., 2007) and show that
406 the ballast-ratio hypothesis (Armstrong et al., 2002; Francois et al., 2002) explained much of the
407 variability of the organic carbon export during upwelling periods. The higher contribution of
408 $CaCO_3$ to the vertical fluxes respect to $bSiO_2$ suggests that carbonate organisms
409 (coccolithophores and foraminifera) must be abundant in the study area. Unfortunately there are

410 no previous studies in the region to corroborate these results. Ecology of coccolithophores has
411 been only studied further south in the Iberian margin where oceanographic conditions are more
412 typically represented by subtropical waters masses influence (Moita et al., 2010; Guerreiro et
413 al., 2013). Otherwise, the slope of the fitted lines point to C_{org} preferentially co-sediment with
414 $bSiO_2$ (Table 4) as occurred in diatom dominated production regimes, where a higher
415 seasonality and a more event-driven export or pulsed sedimentation occurred (Berger and
416 Wefer, 1990).
417 In summary, from our time series of downward particle fluxes we can conclude that ~20% of the
418 particulate C_{org} attributed to primary production sinks on the continental shelf during the low
419 hydrodynamic upwelling period. This means that a large fraction of particulate C_{org} is susceptible
420 to be recycled in the photic layer and/or horizontally exported offshore. Under downwelling
421 conditions (poleward/winter mixing periods) it has been proved that resuspension of underlying
422 sediments, associated to stormy conditions, and intense river discharges regulate the
423 sedimentation processes. Further work is necessary in order to better determine more specific
424 organic matter sources and transport pathways in this highly productive coastal upwelling
425 system.
426

427 **Acknowledgements**

428 The authors gratefully thank the crew of 'R/V Mytilus' for their valuable help during the cruises.
429 The authors also want to specially recognize specific lab work made from different members of
430 both the Oceanography group from the Instituto de Investigaciones Marinas de Vigo (CSIC) and
431 the Divisão de Geologia e Georecursos Marinhos from Instituto Português do Mar e da
432 Atmosfera (IPMA). This study was sponsored by CAIBEX (CTM2007-66408-C02-01/MAR) and
433 REIMAGE (CTM2011–30155–C03–03) projects funded by the Spanish Government, EXCAPA
434 project (10MDS402013PR) supported by Xunta de Galicia, the EU FEDER funded projects
435 RAIA (INTERREG 2009/2011; 0313/RAIA/E) and RAIA.co (INTERREG 2011/2013;
436 052/RAIA.co/1E) and the CALIBERIA project (PTDC/MAR/102045/2008) financed by Fundaçao
437 para a Ciència e a Tecnologia (FCT-Portugal). D.Z. was funded by a postdoctoral fellowship
438 (Plan I2C) from Xunta de Galicia (Spain).
439

440 **References**

441 Alonso-Pérez, F., Ysebaert, T., Castro, C.G., 2010. Effects of suspended mussel culture on
442 benthic-pelagic coupling in a coastal upwelling system (Ría de Vigo, NW Iberian Peninsula). J.
443 Exp. Mar. Biol. Ecol. 382, 2, 96-107.

444 Álvarez-Salgado, X.A., Castro, C.G., Pérez, F.F., Fraga, F., 1997. Nutrient mineralization
445 patterns in shelf waters of the Western Iberian upwelling. Cont. Shel Res. 17(10), 1247-1270.

446 Álvarez-Salgado, X.A., Doval, M.D., Pérez, F.F., 1999. Dissolved organic matter in shelf waters
447 off the Ría de Vigo (NW Iberian upwelling system). J. Mar. Syst. 18, 383-394.

448 Álvarez-Salgado, X.A., Doval, M.D., Borges, A.V., Joint, I., Frankignoulle, M., Woodward,
449 E.M.S., Figueiras, F.G., 2001. Off-shelf fluxes of labile materials by an upwelling filament in the
450 NW Iberian upwelling system. Prog. Oceanogr. 51, 321-337.

451 Álvarez-Salgado, X.A., Figueiras, F.G., Pérez, F.F., Groom, S., Nogueira, E., Borges, A.V.,
452 Chou, L., Castro, C.G., Moncoiffé, G., Ríos, A.F., Miller, A.E.J., Frankignoulle, M., Savidge, G.,
453 Wollast, R., 2003. The Portugal coastal counter current off NW Spain: new insights on its
454 biogeochemical variability. Prog. Oceanogr. 56, 281-321.

455 Antia, A.N., Koeve, K., Fischer, G., Blanz, T., Shulz-Bull, D., Scholten, J., Neuer, S., Kremling,
456 J., Kuss, R., Peinert, D., Hebbeln, D., Bathmann, U., Conte, M., Fehner, U., Zeitzschel, B.,
457 2001. Basin-wide particulate carbon flux in the Atlantic Ocean: Regional export patterns and
458 potential for atmospheric CO_2 sequestration. Global Biogeochem. Cy. 15(4), 845-862.

459 Arístegui, J., Barton, E.D., Álvarez-Salgado, X.A., Santos, A.M.P., Figueiras, F.G., Kifani, S.,
460 Hernández-León, S., Mason, E., Machú, E., Demarcq, H., 2009. Sub-regional ecosystem
461 variability in the Canary Current upwelling. Prog. Oceanogr. 83, 33-48.

462 Armstrong, R.A., Lee, C., Hedges, J.I., Honjo, S., Wakeham, S.G., 2002. A new mechanistic
463 model for organic carbon fluxes in the ocean based on the quantitative association of OC with
464 ballast minerals. Deep-Sea Res. II, 49, 219-236.

465 Bakun, A., 1973. Coastal upwelling Indices, West Coast of North America, 1946-71. US
466 Department of Commerce, National Oceanic and Atmospheric Administration, National Marine
467 Fisheries Service, Seattle, WA.

468 Bauer, J., Cai, W.-J., Raymond, P.A., Bianchi, T.S., Hopkinson, C.S., Regnier, P.A. 2013. The
469 changing carbon cycle of the coastal ocean. Nature 504 61-70.

470 Berger, W., Wefer, G., 1990. Export production: seasonality and intermittency, and
471 paleoceanographic implications. Palaeogeogr. Palaeoclimat. Palaeoecol., 89, 245-254.

472 Biscaye, P.E., Anderson, R.F., 1994. Fluxes of particulate matter on the slope of the southern
473 Middle Atlantic Bight: SEEP-II. Deep-Sea Res. 41(2/3), 459-509.

474 Bode, A., Varela, M., Barquero, S., Alvarez-Osorio, M.T., Gonzalez, N., 1998. Preliminary
475 studies on the export of organic matter during phytoplankton blooms off La Coruña
476 (Northwestern Spain). J. Mar. Biol. 78 (1), 1-15.

477 Castro, C.G., Álvarez-Salgado, X.A., Figueiras, F.G., Pérez, F.F., Fraga, F., 1997. Transient
478 hydrographic and chemical conditions affecting microplankton populations in the coastal
479 transitions zone of the Iberian upwelling system (NW Spain) in September 1986. J. Mar. Res.
480 55, 321-352.

481 Castro, C.G., Pérez, F.F., Álvarez-Salgado, X.A., Fraga, F., 2000. Coupling between
482 thermohaline, chemical and biological fields during two contrasting upwelling events off the NW
483 Iberian Peninsula. Cont. Shelf Res. 20, 189-210.

484 Castro, C.G., Nieto-Cid, M., Álvarez-Salgado, X.A., Pérez, F.F., 2006. Local remineralization
485 patterns in the mesopelagic zone of the Eastern North Atlantic, off the NW Iberian Peninsula.
486 Deep-Sea Res. I, 53, 1925-1940.

487 Chavez, F., Messié, M., Pennington, J. T. 2011. Marine primary production in relation to climate
488 variability and change Annu. Rev. Mar. Sci. 3, 227 -260.

489 Dias, J.M.A., González, R., García, C., Díaz-del-Río, V., 2002. Sediment distribution patterns on
490 the Galicia–Minho continental shelf. Prog. Oceanogr. 52 (2–4), 215–231.

491 Espinoza-Gonzalez, O., Figueiras, F.G., Crespo, B., Teixeira, I.G., Castro, C.G., 2012.
492 Autotrophic and heterotrophic microbial plankton biomass in the NW Iberian upwelling: seasonal
493 assessment of metabolic balance. Aquat. Microb. Ecol. 67, 77-89.

494 Figueiras, F.G., Ríos, A.F., 1993. Phytoplankton succession, red tides and the hydrographic
495 regime in the Rías Bajas of Galicia. In: Smayda, T.J., Shimizu, Y. (Eds.), Toxic phytoplankton
496 blooms in the Sea. Elsevier, New York, pp. 239-244.

497 Filgueira, R., Castro, B.G., 2011. Study of the trophic web of San Simón Bay (Ría de Vigo) by
498 using stable isotopes. Cont. Shelf Res. 31, 476-487.

499 Fischer, G., Karakas, G., Blaas, M., Ratmeyer, V., Nowald, N., Schlitzer, P., Helmke, P.,
500 Davenport, R., Donner, B., Neuer, S., Wefer, G., 2009. Mineral ballast and particle settling rates
501 in the coastal upwelling system off NW Africa and South Atlantic. Int. J. Earth Sci. 98, 281-298.

502 Fraga, F., 1981. Upwelling off the Galician coast, nothwest of Spain. In: Richards, F. (Ed.),
503 Coastal Upwelling. American Geophysical Union, Washington, pp. 176-182.

504 Fraga, F., Ríos, A.F., Pérez, F.F., Figueiras, F.G., 1998. Theoretical limits of oxygen: carbon
505 and oxygen:nitrogen ratios during photosynthesis and mineralisation of organic matter in the
506 sea. Sci. Mar. 62(1), 161-168.

507 Francois, R., Honjo, S., Krishfield, R., Manganini, S., 2002. Factors controlling the flux of
508 organic carbon to the bathypelagic zone of the ocean. Global Biogeochem. Cy. 16(4), 1087,
509 doi:10.1029/2001GB001722.

510 Gago, J., Gilcoto, M., Pérez, F.F., Ríos, A.F., 2003. Short-term variability of fCO_2 in seawater
511 and air–sea CO_2 fluxes in a coastal upwelling system (Ría de Vigo, NW Spain). Mar. Chem. 80,
512 247-264.

García-Muñoz, M., Arístegui, J., Pelegrí, J.L., Antoranz, A., Ojeda, A., Torres, M., 2005. Exchange of carbon by an upwelling filament off Cape Guir (NW Africa). J. Mar. Sys. 54, 83-95.

Gardner, W.D., Biscaye, P.E., Richardson, M.J., 1997. A sediment trap experiment in the Vema Channel to evaluate the effect of horizontal particle fluxes on measured vertical fluxes. J. Mar. Res., 55, 995-1028.

Goñi, M.A., Aceves, H.L., Thunell, R.C., Tappa, E., Black, D., Astor, Y., Varela, R., Muller-Kager, F., 2003. Biogenic fluxes in the Cariaco Basin: a combined study of sinking particulates and underlying sediments. Deep Sea Res. I, 50, 781-807.

Guerreiro, C., Oliveira, A., de Stigter, H., Cachao, M., Sá, C., Borges, C., Cros, L., Santos, A., Fortuño, J.M., Rodrigues, A., 2013. Late winter coccolithophore bloom off central Portugal in response to river discharge and upwelling. Cont. Shelf Res. 59, 65-83.

Hansen, H.P. and Grassoff, K., 1983. Automated chemical analysis. In: Grasshoff, K., Ehrhadt, M., and Kremling, K. (Eds). Methods of seawater analysis. Verlag Chemie, Weinheim, p.p. 347-395.

Haynes, R., Barton, E.D., 1990. A poleward flow along the Atlantic coast of the Iberian Peninsula. J. Geophys. Res. 95, 11425-11442.

Haynes, R., Barton, E.D., Pilling, I., 1993. Development, persistence, and variability of upwelling filaments off the Atlantic coast of the Iberian Peninsula. J. Geophys. Res. 98 (C12), 22681-22692.

Heussner, S., Ratti, C., Carbonne, J., 1990. The PPS 3 time-series sediment trap and the trap sample techniques used during the ECOMARGE experiment. Cont.Shelf Res. 10, 943-958.

Heussner, S., Durrieu du Madron, X., Calafat, A., Canals, M., Carbonne, J., Delsaut, N., Saragoni, G., 2006. Spatial and temporal variability of downward particle fluxes on a continental slope: Lessons from an 8-yr experiment in the Gulf of Lions (NW Mediterranean). Mar. Geol. 234, 63-92.

538 Honjo, S., Manganini, S.J., Krishfield, R.A., Francois, R., 2008. Particulate organic carbon
539 fluxes to the ocean interior and factors controlling the biological pump: A synthesis of global
540 sediment trap programs since 1983. Progr. Oceanogr. 76, 217-285.

541 JGOFS. Global biogeochemistry and global change. IGBP Science No. 2.: ISSN 1650-7770.

542 Joint, I., Inall, M., Torres, R., Figueiras, F.G., Álvarez-Salgado, X.A., Rees, A.P., Malcolm, E.,
543 Woodward, E.M.S., 2001. Two Lagrangian experiments in the Iberian Upwelling System:
544 tracking an upwelling event and an off-shore filament. Prog. Oceanogr. 51, 221-248.

545 Liu, K. K., Atkinson, L., Quiñones, R., and Talaue-McManus, L. 2010 Carbon and Nutrient
546 fluxes in continental margins: a global synthesis,Springer-Verlag, Berlin Heidelberg.

547 Lutz, M., Dunbar, R., Caldeira, K., 2002. Regional variability in the vertical flux of particulate
548 organic carbon in the ocean interior. Global Biogeochem. Cy. 16(3), 1-11.

549 Martin, J.H., Knauer, G.A., Karl, D.M., Broenkow, W.W., 1987. VERTEX: carbon cycling in the
550 northeast Pacific. Deep-Sea Res. 34 (2), 267-285.

551 Moita, T.M., Silva, A., Palma, S., Vilarinho, M.G., 2010. The coccolithophore summer-autumn
552 assemblage in the upwelling waters of Portugal: Patterns of mesoscale distribution (1985-2005).
553 Estuar. Coast Shelf S. 87, 411-419.

554 Mortlock, R.A., Froelich, P.N., 1989. A simple method for the rapid determinations of biogenic
555 opal in pelagic marine sediments. Deep Sea Res. 36 (9), 1415–1426.

556 Muller-Karger, F. E., Varela, R., Thunell, R., Luerssen, R., Hu, C., Walsh, J. J. 2005. The
557 importance of continental margins in the global carbon cycle, Geophys. Res. Lett. 31(1), 1-4.

558 Oliveira, A., Rocha, F., Rodrigues, A., Jouanneau, J., Dias, A., Weber, O., Gomes, C., 2002.
559 Clay minerals from the sedimentary cover from the Northwest Iberian shelf. Prog. Oceanogr. 52,
560 233-247.

561 Olli, K., Wexels Riser, C., Wassmann, P., Ratkova, T., Arashkevich, E., Pasternak, A., 2001.
562 Vertical flux of biogenic matter during a Lagrangian study off the NW Spanish continental
563 margin. Prog. Oceanogr. 51 (2-4), 443-466.

564 Otero, P., Ruiz-Villarreal, M., Peliz,A., Cabanas, J.M., 2010. Climatology and reconstruction of
565 runoff time series in northwest Iberia: influence in the shelf buoyancy budget off Ría de Vigo.
566 Sci. Mar. 74 (2), 247-266.

567 Peña, M.A., Denman, K.L., Forber, J.R., Calvert, S.E., Thomson, R.E., 1996. Sinking particle
568 fluxes from the euphotic zone over the continental slope of an eastern boundary current region.
569 J. Mar. Res. 54, 1097-1122.

570 Piedracoba, S., Nieto-Cid, M., Teixeira, I.G., Garrido, J.L., Álvarez-Salgado, X.A., Rosón, G.,
571 Castro, C.G., Pérez, F.F., 2008. Physical–biological coupling in the coastal upwelling system of
572 the Ría de Vigo (NW Spain). II: *In vitro* approach. Mar. Ecol. Prog. Ser. 353, 41-53.

573 Pilskaln, C.H., Paduan, J.B., Chavez, F.P., Anderson, R.Y., Berelson, W., 1996. Carbon export
574 and regeneration in the coastal upwelling system of Monterey Bay, central California. J. Mar.
575 Res. 54, 1149-1178.

576 Redfield; A.C., 1958. The biological control of chemical factors in the environment. Am. Sci.
577 46(3), pp. 230A, 205-221.

578 Schmidt, F., Hinrichs, K.U., Elvert, M., 2010. Sources, transport and partitioning of organic
579 matter at a highly dynamic continental margin. Mar. Chem. 118, 37-55.

580 Suess, E., 1980. Particulate organic carbon flux in the oceans-surface productivity and oxygen
581 utilization. Nature, 288, 260-263.

582 Tenore, K. R., Alonso-Noval, M., Álvarez -Ossorio, M., Atkinson, L.P., Cabanas, J. M., Cal,
583 R.M., Campos, H.J., Castillejo, F., Chesney, E.J., González, N., Hanson, R.B., McClain, C.R.,
584 Miranda, A., Roman, M.R., Sánchez, J., Santiago, G., Valdes, L., Varela, M., Yoder, J., 1995.
585 Fisheries and oceanography off Galicia, NW Spain: Mesoscale spatial and temporal changes in

586 physical processes and resultant patterns of biological productivity. J. Geophys. Res. 100(C6),
587 10943-10966.

588 Thunell, R.C., 1998. Particle fluxes in a coastal upwelling zone: sediment trap results from
589 Santa Barbara Basin, California. Deep-Sea Res. II, 45, 1863-1884.

590 Thunell, R., Benitez-Nelson, C., Varela, R., Astor, Y., Muller-Karger, F., 2007. Particulate
591 organic carbon fluxes algong upwelling-dominated continental margins: Rates and mechanisms.
592 Global Biogeochem. Cy. 21, GB1022, doi: 10.1029/2006GB002793.

593 van Weering, T.C.E., Stigter, H.C., Boer, W., Haas, H., 2002. Recent sediment transport and
594 accumulation on the NW Iberian margin. Prog. Oceanogr. 52, 349-371.

595 Varela, M., Prego, R., Pazos, Y., 2004. Vertical biogenic particle flux in a western Galician ria
596 (NW Iberian Peninsula). Mar. Ecol-Prog. Ser. 269, 17-32.

597 Vitorino, J., Oliveira, A., Jouanneau, J.M., Drago, T., 2002. Winter dynamics on the northern
598 Portuguese shelf. Part 2: bottom boundary layers and sediment dispersal. Progr. Oceanogr. 52
599 (2–4), 155–170.

600 Walsh, J.J., 1981. A carbon budget for overfishing off Peru. Nature, 290, 300-304.

601 Wollast, R. 1998. Evaluation and comparison of the global carbon cycle in the coastal zone and
602 in the open ocean In The Global Coastal Ocean (Brink K.H. & Robinson, A.R. eds), John Wiley
603 & Sons, Inc., 213-252.

604 Wooster, W.S., Bakun, A., McLain, D.R.,1976. The seasonal upwelling cycle along the eastern
605 boundary of the North Atlantic. J. Mar. Res. 34, 131−141.

606 Yentsch, C.S., and Menzel,D.W., 1963. A method for the determination of phytoplankton
607 chlorophyll and phaeophytin by fluorescence. Deep Sea Res. 10, 221-231.

608 Zúñiga, D., Alonso-Perez, F., Castro, C.G., Arbones, B., Figueiras, F., 2011. Seasonal
609 contribution of living phytoplankton carbón to vertical fluxes in a coastal upwellig system (Ría de
610 Vigo, NW Spain). Cont. Shelf Res. 31, 414-424.

611

612

613

614 **Figure captions**

615 Figure 1. Map of the NW Iberian Peninsula continental margin showing the position of the
616 mooring line (RAIA) site and the WANA hindcast reanalysis points 3027034 ($WANA_S$ off Cape
617 Silleiro) and 1044067 ($WANA_G$ off A Guarda) from which wave data were obtained. Circulation
618 pattern along the margin is also presented. It includes the coastal current (solid line) moving
619 southwards under upwelling favourable conditions, and the northward advection of southerly
620 waters by the Iberian Poleward Current (IPC) (dashed line) dominating during downwelling
621 periods.

622 Figure 2. Bottom-tethered mooring diagram deployed at the RAIA station showing main
623 oceanographic instrumentation attached to the mooring line. The drawing is not to scale.

624 Figure 3. Time-series of (a) upwelling index ($-Q_x$), (b) Minho and Douro river discharges and (c)
625 significant wave height (H_S) obtained for propagation from the $WANA_S$ (off Silleiro) and $WANA_G$
626 (off A Guarda) points.

627 Figure 4. Time-series of (a) temperature, (b) salinity), (c) nitrate (NO_3^-), (d) Chlorophyll *a* (Chl *a*)
628 and (e) turbidity concentrations registered at RAIA station. U: upwelling; P: Poleward; M: mixing;
629 n.d.: no data.

630 Figure 5. Time-series of total (TMF) and major constituent (OM: organic matter; $CaCO_3$: calcium
631 carbonate; $bSiO_2$: biogenic opal and Litho: Lithogenic) mass fluxes registered at RAIA station.
632 U: upwelling; P: Poleward; M: mixing; n.d.: no data. Numbers are used to highlight main particle
633 flux periods.

634 Figure 6. Relative contributions (in percentage) of major compounds (OM: organic matter;
635 $CaCO_3$: calcium carbonate; $bSiO_2$: biogenic opal and Litho: Lithogenic) to the total mass fluxes
636 (TMF) of the settling material collected by the RAIA sediment trap. U: upwelling; P: Poleward;
637 M: mixing; n.d.: no data. Numbers are used to highlight main particle flux periods.

638 Figure 7: Time-series of Minho (solid line) and Douro (dashed line) river discharges, and organic
639 carbon (C_{org}) /total nitrogen (TN) atomic ratio (white dots) of the sinking particles collected by the
640 RAIA sediment trap. Carbon isotopic ($\delta^{13}C_{org}$) signals (black dots) of several sediment trap
641 samples are also presented. Lowest $\delta^{13}C_{org}$ signal (-21.6‰) characteristic of marine particulate

642 organic matter in the adjacent Ría de Vigo (Filgueira and Castro, 2011) is marked by a dashed
643 line in the figure. U: upwelling; P: Poleward; M: mixing; n.d.: no data. Numbers are used to
644 highlight main particle flux periods.
645 Figure 8: Time-series of lithogenic fluxes (white dots) at RAIA station and significant wave
646 height (H_S) at $WANA_S$ off Silleiro (solid line) and $WANA_G$ off A Guarda (dashed line) points. U:
647 upwelling; P: Poleward; M: mixing; n.d.: no data. Numbers are used to highlight main particle
648 flux periods.
649 Figure 9. Scatter plot of photic zone integrated chlorophyll *a* (Chl *a*) vs. Ekman transport ($-Q_x$)
650 (same day as Chl *a* sampling). Dot color scale represents organic carbon (C_{org}) fluxes registered
651 by the sediment trap including the day of Chl *a* sampling. Dot numbers are referred to C_{org} flux
652 events identified during upwelling periods (as referred in Figure 5). Unfortunately, there were no
653 Chl *a* data for event 14.
654

655 Table 1. Recorded days and sampling intervals of the mooring deployments at RAIA station.

656

Period	Deployment	Recovery	Sampling interval (days)	Observations
I	5 Nov 08	12 Feb 09	9	Ok
II	25 Mar 09	4 Jun 09	9	Lost
III	12 Jun 09	21 Sep 09	4-12	Ok
IV	24 Sep 09	11 Dec 09	9	Ok
V	28 Jan 10	27 Apr 10	9-12	Ok
VI	29 Jun 10	4 Dec 10	9	Lost
VII	26 Jan 11	28 Apr 11	7	Ok
VIII	10 Jun 11	14 Oct 11	7	Ok
IX	12 Jan 12	20 Jun 12	7	Ok

657

658

659 Table 2. Mean statistical parameters for ADCP current speeds registered at 45 m water depth
660 and trap tilt angle obtained from CTD pressure data (November 2008-May 2010). S.D. refers to
661 the standard deviation of the current speed. Unfortunately, data from from June 2010 to June
662 2012 were not recorded.
663

	Days	Average cm s^{-1} (S.D.)	Maximum speed cm s^{-1}	Speed < 20 $(\%)^{-1}$	Tilt < 5º (%)	Tilt < 10º (%)
Upwelling	198	10.5 (6.8)	41.0	94	76	92
Poleward	183	13.3 (10.6)	62.7	85	57	82
Mixing	63	15.4 (10.6)	66.7	76	87	98

664
665

666 Table 3. Total and seasonal (upwelling; poleward; mixing) mean (standard deviation) values of both total (TMF) and major compounds (OM: organic matter;

667 $CaCO_3$: calcium carbonate; $bSiO_2$: biogenic opal and Litho: lithogenic) mass fluxes and percentages. Bio: total biogenic contribution (OM, $CaCO_3$ and $bSiO_2$).

668 Organic carbon (C_{org}) / total nitrogen (TN) atomic ratio is also presented.

669

	TMF ($g\ m^{-2}\ d^{-1}$)	OM (%)	OM flux ($mg\ m^{-2}\ d^{-1}$)	C_{org}/TN (mol:mol)	$CaCO_3$ (%)	$CaCO_3$ ($mg\ m^{-2}\ d^{-1}$)	$bSiO_2$ (%)	$bSiO_2$ ($mg\ m^{-2}\ d^{-1}$)	Bio (%)	Bio flux ($g\ m^{-2}\ d^{-1}$)	Litho (%)	Litho flux ($g\ m^{-2}\ d^{-1}$)
Upwelling	3.6 (4.1)	13.2 (5.7)	404 (400)	8.9 (0.7)	10.3 (5.9)	441 (531)	5.9 (2.0)	245 (265)	30 (7)	1.2 (1.2)	69.8 (7.0)	2.9 (3.0)
Poleward	12.9 (9.6)	9.7 (4.8)	935 (564)	9.9 (0.8)	8.0 (2.4)	1235 (877)	3.2 (0.8)	479 (286)	19.6 (3.4)	2.9 (1.6)	80.4 (3.4)	12.2 (7.3)
Mixing	5.6 (5.6)	7.7 (2.1)	366 (327)	9.9 (0.8)	7.8 (2.8)	453 (474)	3.5 (1.2)	175 (147)	18.9 (3.3)	1.0 (0.9)	80.9 (3.2)	4.7 (4.7)
Total	5.5 (6.3)	10.9 (5.4)	458 (446)	9.3 (0.9)	9.3 (4.9)	542 (623)	4.8 (2.0)	263 (254)	24.8 (8.3)	1.4 (1.3)	74.6 (7.8)	4.7 (5.2)

Table 4. Linear regression correlation coefficients for organic carbon (C_{org}) flux versus total mass (TMF), biomineral (calcium carbonate: $CaCO_3$ and biogenic opal: $bSiO_2$) and lithogenic (Litho) fluxes for the upwelling period. All correlation coefficients (r) are significat ($P< 0.001$). Regression line slope between the different compounds is also shown. Number of samples used for the linear regressions: 49.

	r	Slope
TMF	0.95	0.05
$CaCO_3$	0.96	0.36
$bSiO_2$	0.96	0.78
Litho	0.90	0.06

682 Figure 1

683

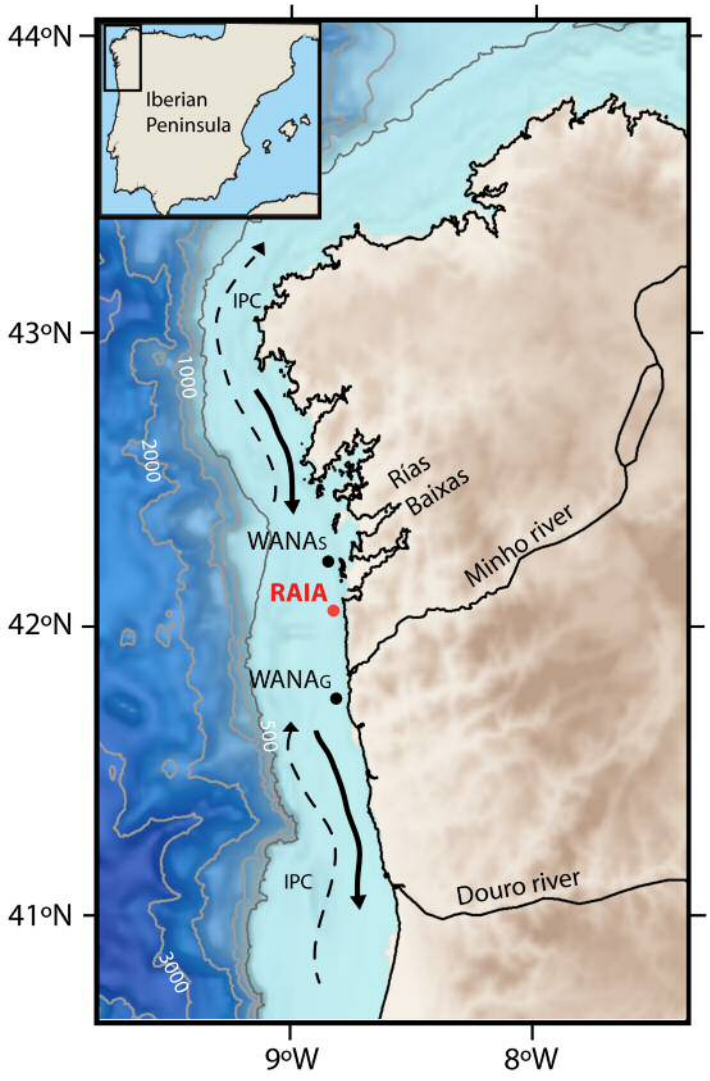

684

685

686

687 Figure 2

688

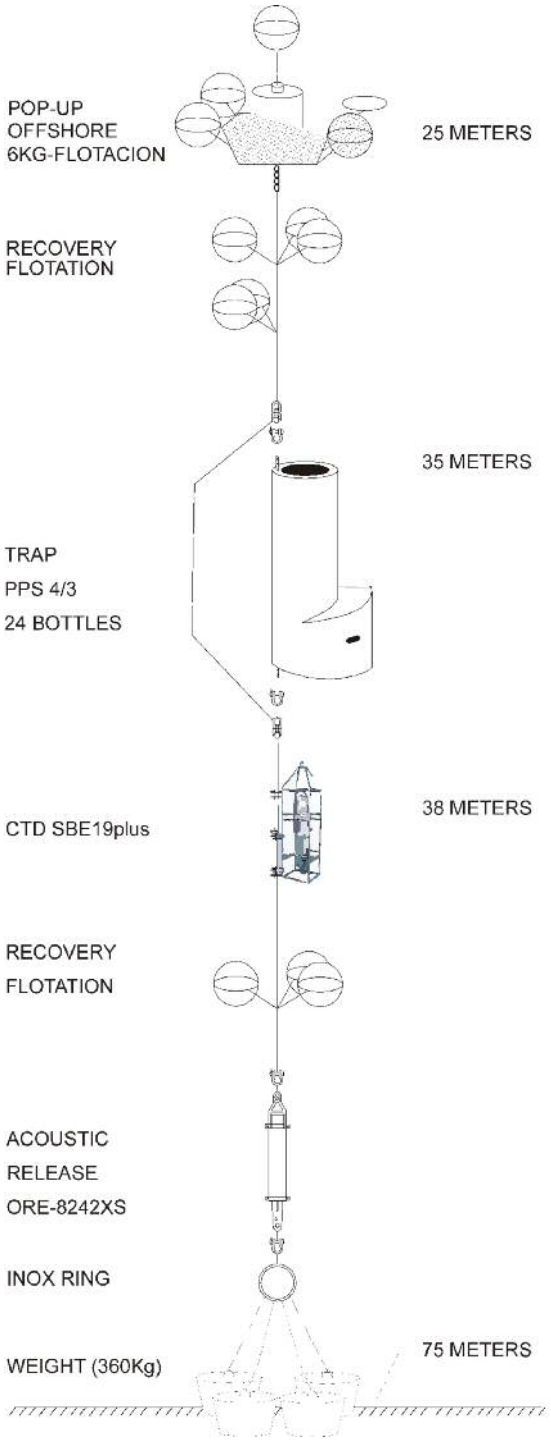

689

690

691

692 Figure 3

693

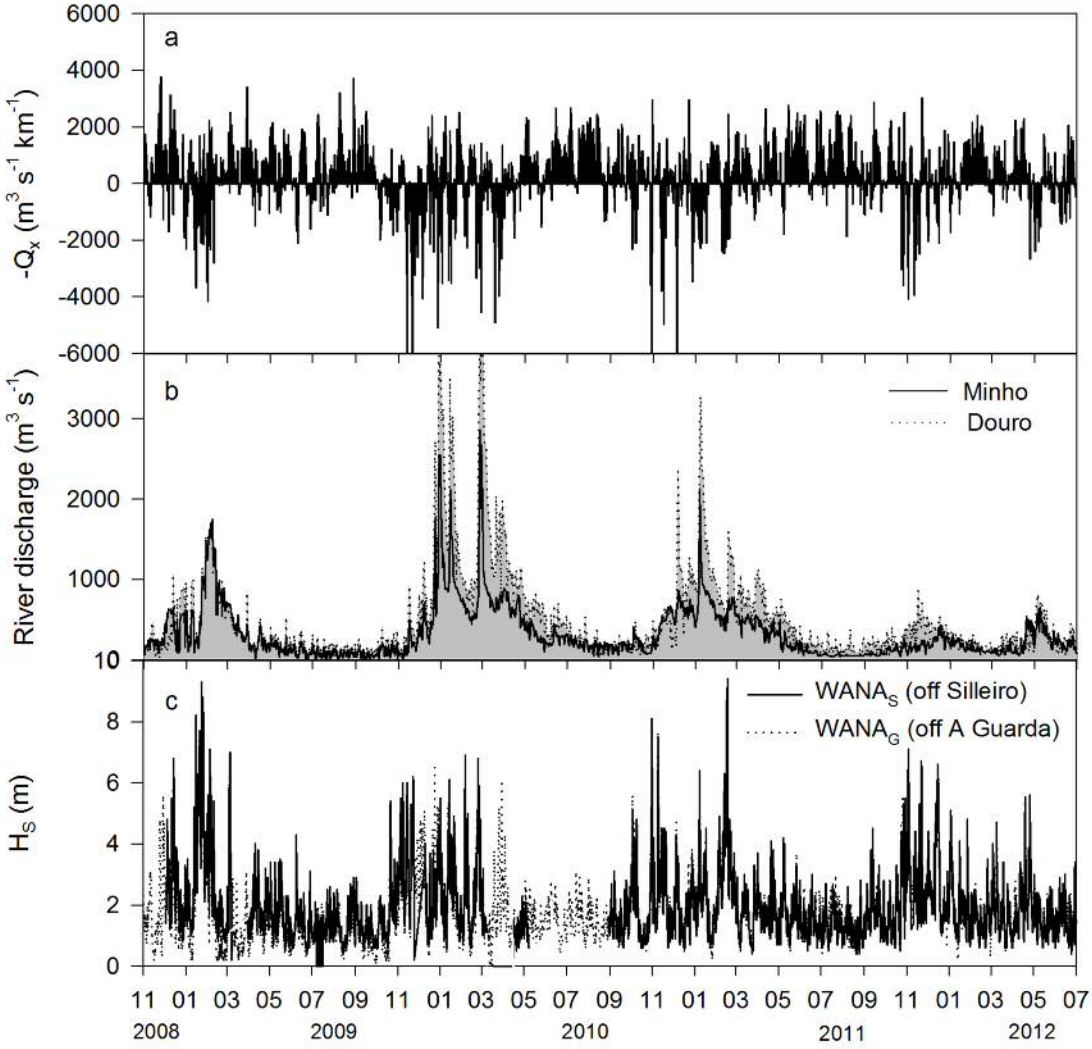

694

695

696

697 Figure 4

698

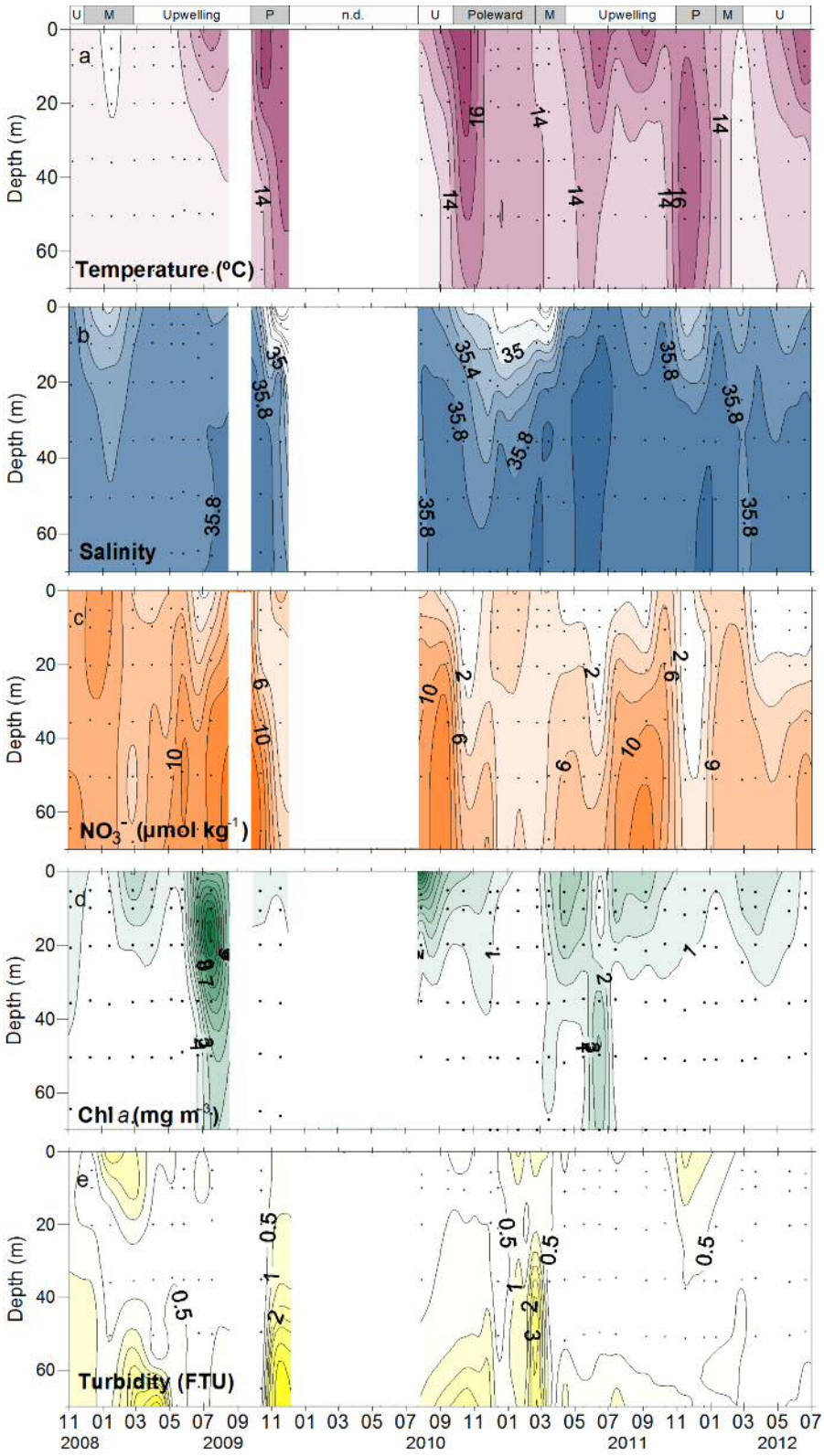

699

700

701 Figure 5

702

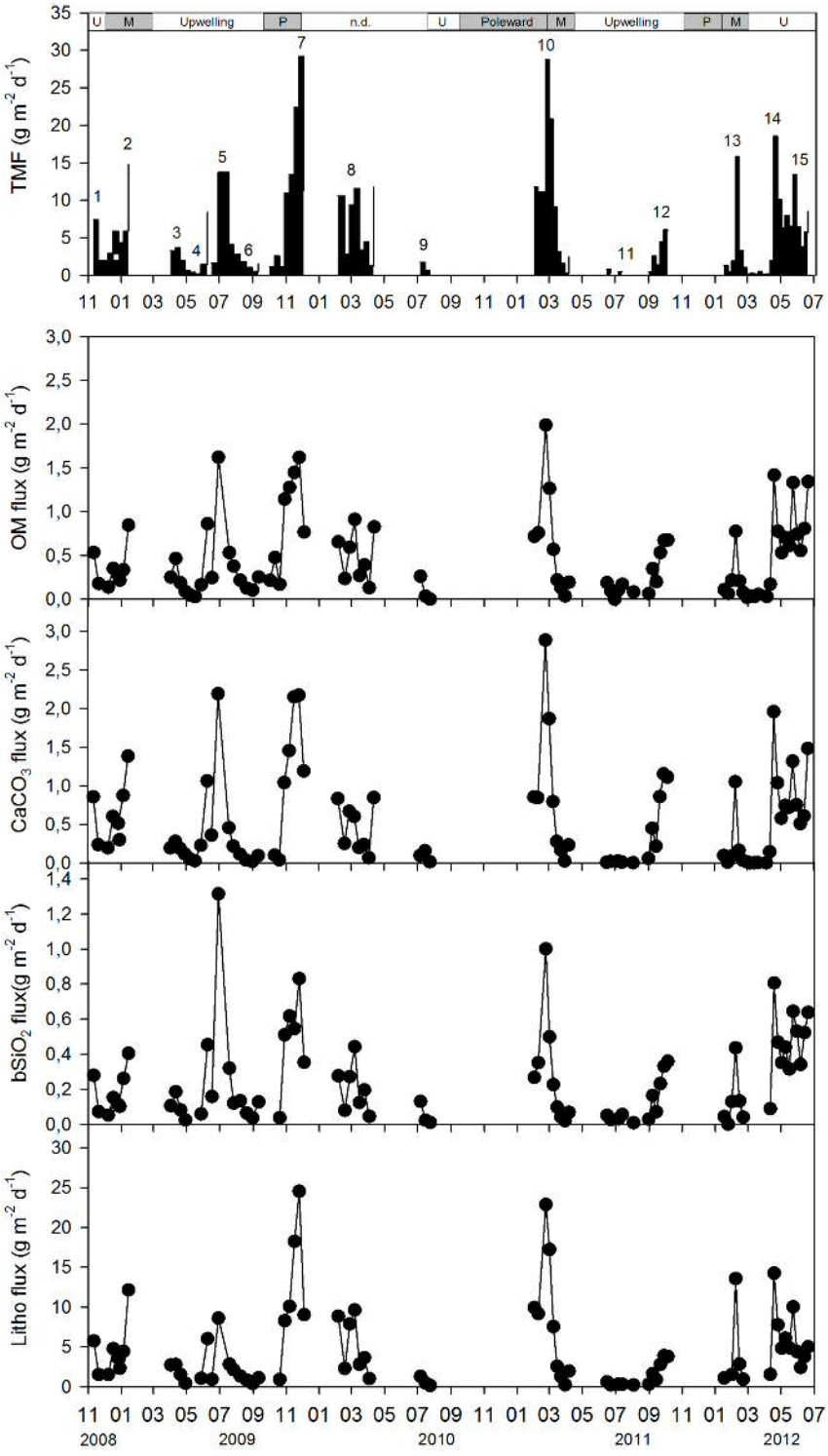

703

704

705

706 Figure 6

707

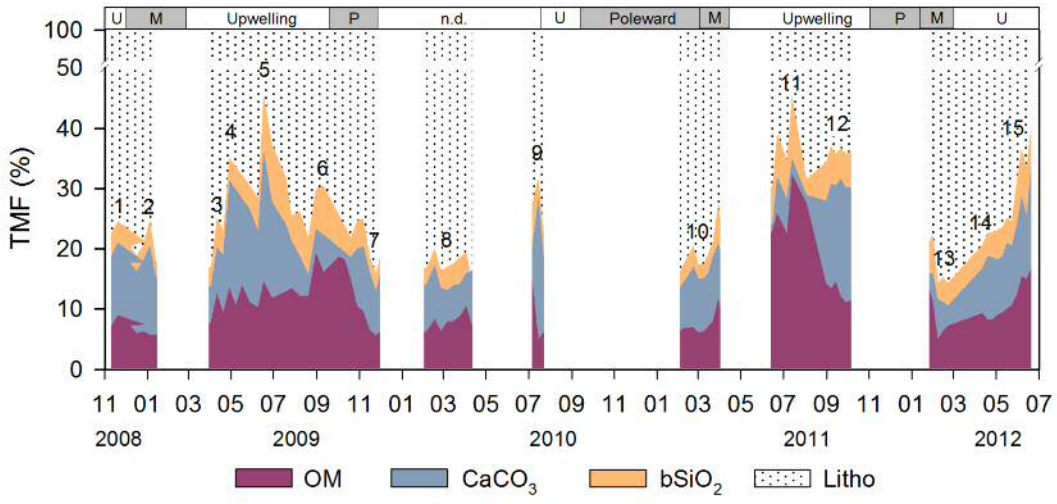

708

709

710

711 Figure 7

712

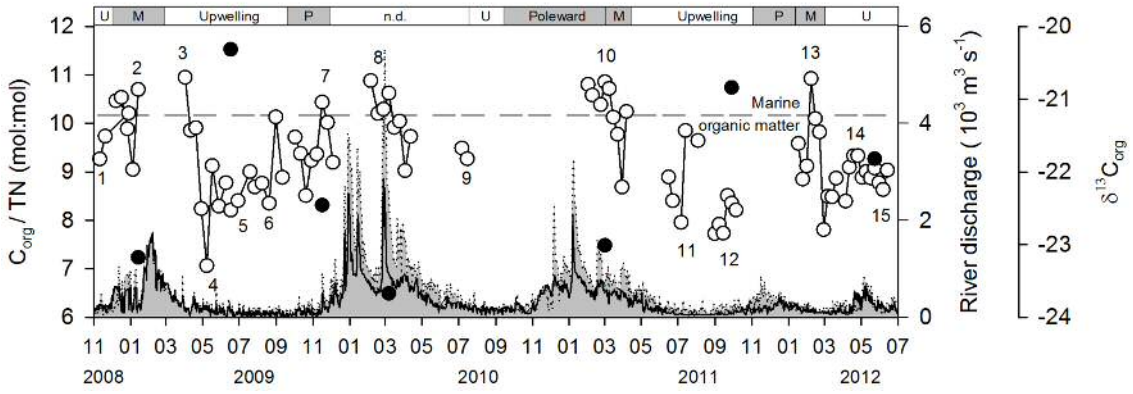

713

714

715

716 Figure 8

717

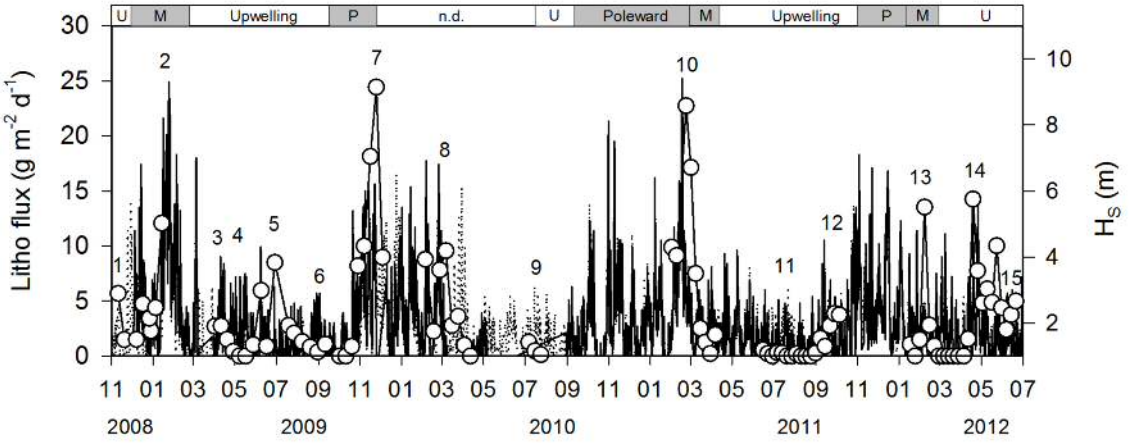

718

719

720

721 Figure 9

722

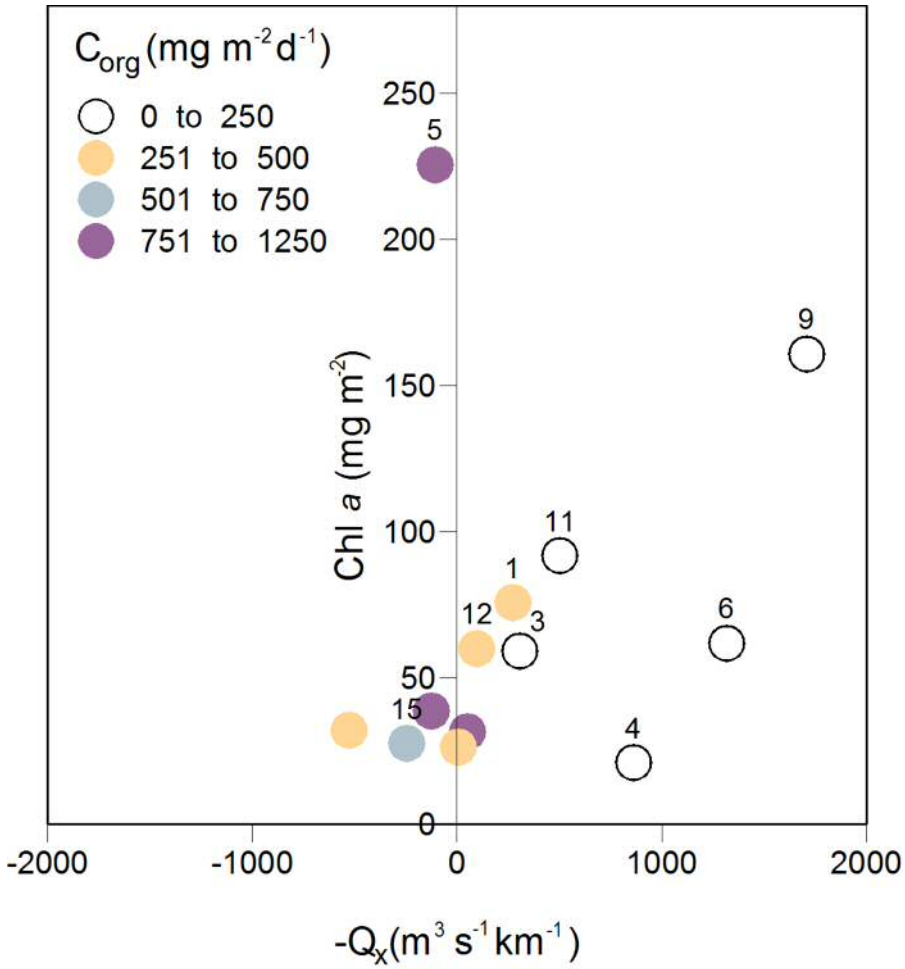

723